PLASMA DYNAMICS

IX. PLASMA PHYSICS*

Prof. S. C. Brown
Prof. W. P. Allis
Prof. G. Bekefi
Prof. D. R. Whitehouse
Dr. J. C. Ingraham
Dr. G. Lampis
M. L. Andrews
F. X. Crist
J. K. Domen
E. W. Fitzgerald, Jr.
D. L. Flannery
E. V. George
W. H. Glenn, Jr.
E. B. Hooper, Jr.
P. W. Jameson
R. L. Kronquist
D. T. Llewellyn-Jones
E. M. Mattison
J. J. McCarthy
W. J. Mulligan
J. J. Nolan, Jr.
R. C. Owen
L. D. Pleasance
G. L. Rogoff
D. W. Swain
F. Y-F. Tse

A. ELECTRON DENSITY MEASUREMENTS WITH A LASER INTERFEROMETER

A laser interferometer has been used to study the time and spatial decay of a pulsed P.I.G. discharge.[1] The electron density decay is studied in a range from above 10^{14} cm^{-3} to below 10^{13} cm^{-3}. It is concluded from the dependence of the decay on gas pressure and magnetic field that the electron density and temperature both decay initially by radial diffusion. After a time of 100-200 microseconds, electron-ion collisions become an important cooling mechanism, and the electron temperature drops rapidly. The decay rates after 200 microseconds are consistent with the radiative-collision calculations of Bates, et al.[2]

The interferometer used in the study has been described elsewhere.[3] Briefly, it can measure phase shifts in the optical and near infrared of less than $2\pi \times 10^{-3}$ radians. In the present plasma, electron densities are thus measured with an accuracy of 10^{12} cm^{-3}. The time response of the interferometer was measured to be less than 5 microseconds.

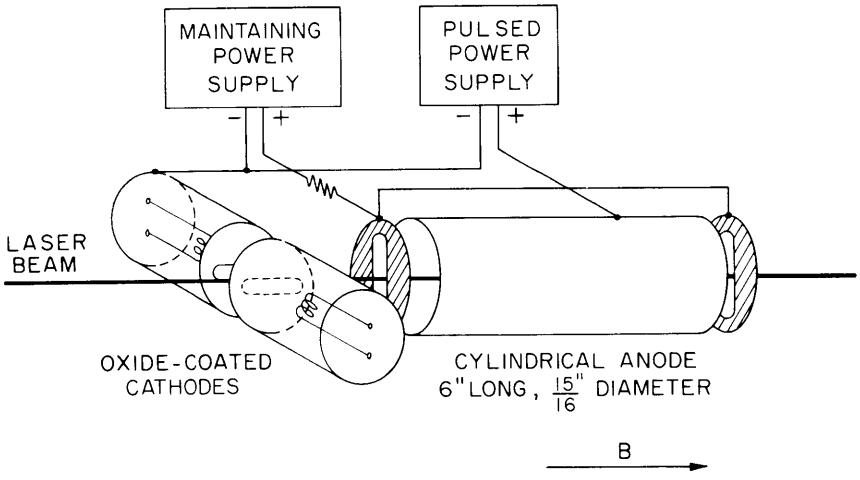

Fig. IX-1. The P.I.G. discharge.

*This work was supported principally by the U.S. Atomic Energy Commission under Contract AT(30-1)-1842.

The discharge tube is shown in Fig. IX-1. Cathodes have been placed outside the discharge region so that the laser beam can pass along the axis of the tube. A current pulse containing approximately one joule was fired 100 times per second by means of a delay line. To make the pulse reproducible the gas was pre-ionized by running a weak (10 ma) DC discharge.

Examples of the time and spatial dependence of the electron density are shown in Fig. IX-2. As can be seen the density closely follows the Bessel function predicted by elementary diffusion theory.

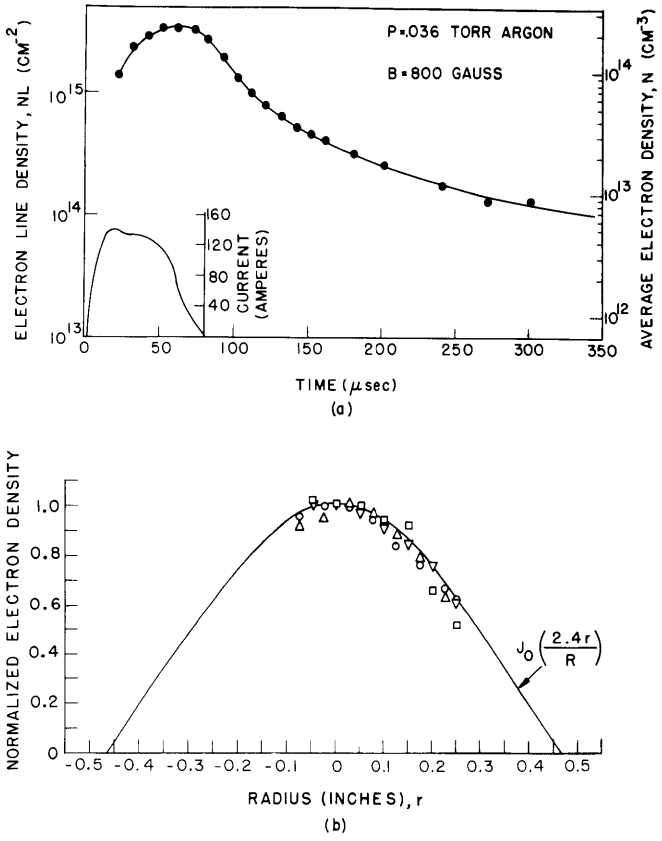

Fig. IX-2.

(a) Time decay of the axial electron density. The discharge current is shown in the lower left-hand corner.

(b) Radial distribution of the electron density. The data is compared with the zero-order Bessel function. The magnetic field is 800 gauss, and the time t = 80 μsec; similar data were obtained at other fields and times in the afterglow. The symbols correspond to different pressures: □, p = 0.22 Torr; ○, p = 0.044 Torr; △, p = 0.104 Torr; ▽, p = 0.160 Torr.

The rate of change of the electron density is plotted in Fig. IX-3 for several pressures. It is clear from this figure that in the early afterglow the decay is most rapid for low pressures. This fact and the spatial dependence (Fig. IX-2b) are strong indications that the initial decay is by diffusion. In addition, the magnetic field dependence (not shown) indicates that diffusion across the field dominates diffusion along the field, a conclusion which is supported by numerical estimates of decay rates.

To obtain a detailed picture of the decay of the plasma, it is necessary to consider both temperature and density decay. As the density decay in the early afterglow is

primarily due to diffusion, the density decay equation is

$$\frac{\partial \ln n}{\partial t} = -\frac{D_{am}}{\Lambda^2} \tag{1}$$

Here D_{am} is the coefficient for ambipolar diffusion across the magnetic field:

$$D_{am} = \frac{D_a}{1 + \frac{\omega_e \omega_i}{\nu_{ei} \nu_{ia}}} \tag{2}$$

where ω_e and ω_i are the electron and ion cyclotron frequencies, ν_{ia} is the ion-atom collision frequency, and ν_{ei} is a spatially averaged electron-ion collision frequency.

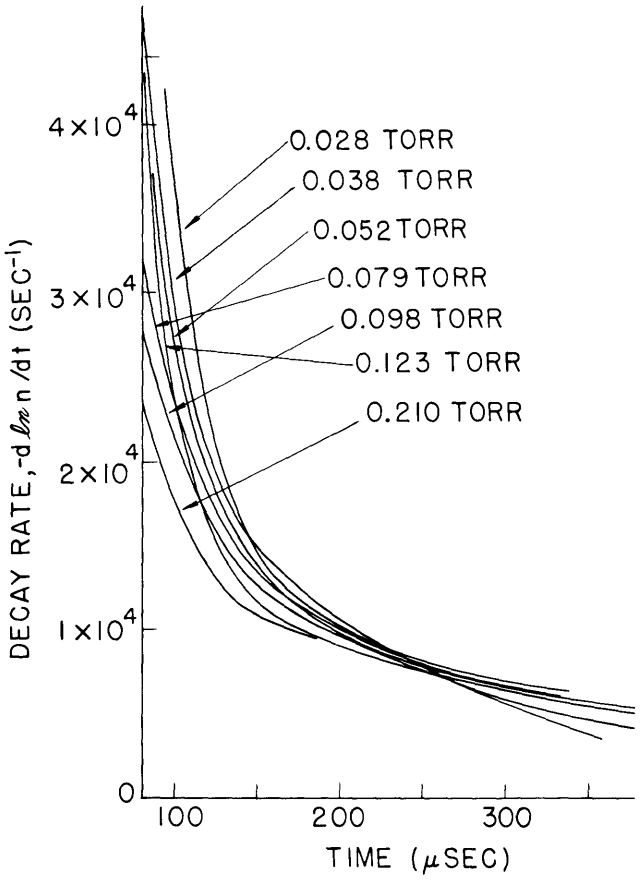

Fig. IX-3.

Plasma decay rates as a function of time. The magnetic field is 800 gauss. The experimental points are not shown because of lack of space, instead smooth curves have been drawn through the data.

Following Golant and Zhilinskii,[4] ν_{ei} is found to be 0.38 times the collision frequency at the center of the discharge tube.

Calculations of the electron and ion cooling rates were made.[1] It was found that the

ion-atom collision frequency is so high that the ions are at practically the atom temperature. The important electron cooling mechanisms are diffusion and electron-ion collisions. Recombination plays no part at these densities and temperatures. The rate of electron temperature decay is given by

$$\frac{\partial \ln T}{\partial t} = -\frac{D_{am}}{\Lambda^2}\left[\frac{2}{3} + \frac{1-(\omega_e/\nu_{ei})^2}{1+(\omega_e/\nu_{ei})^2} + \frac{2}{3}\,\frac{a}{1+\dfrac{\omega_e\omega_i}{\nu_{ei}\nu_{ia}}} + \frac{2}{3}\,b\right] - g\nu_{ei}. \tag{3}$$

The terms in the brackets on the right-hand side of Eq. 3 arise in the order presented from (a) the temperature dependence of the ambipolar diffusion coefficient; (b) the temperature dependence of the electron mobility; and (c) the flow of diffusion currents in the space-charge fields. The term containing "a" arises from the volume field and that containing "b" arises from sheath fields. Both "a" and "b" are weak functions of the plasma parameters; for the present plasma they are about 2.1 and 0.16 respectively. The collisional cooling term is proportional to $g = 2m_e/M_A$.

As diffusion is important for both the density and the temperature decays, it is convenient to combine Eqs. 2 and 3:

$$\frac{\partial \ln (T^{3/2}/n)}{\partial t} = -\frac{D_{am}}{\Lambda^2}\left[\frac{3}{2}\,\frac{1-(\omega_e/\nu_{ei})^2}{1+(\omega_e/\nu_{ei})^2} + \frac{a}{1+\dfrac{\omega_e\omega_i}{\nu_{ei}\nu_{ia}}} + b\right] - \frac{3}{2}\,g\nu_{ei}. \tag{4}$$

The right-hand side of this equation can be either positive or negative. In the limiting case that it is zero, $T^{3/2}/n$ is a constant during the decay. In this case, the density decay equation becomes

$$\frac{\partial \ln n}{\partial t} = -\left(\frac{D_{am}}{\Lambda^2}\right)\left(\frac{n}{n_o}\right)^{2/3} \tag{5}$$

where the subscript zero indicates initial conditions.

Examples of the decay rates of the plasma are plotted in Fig. IX-4 for a magnetic field of 800 gauss. It is observed that the initial decay of the plasma follows Eq. 5, indicating that the right-hand side of Eq. 4 is indeed approximately zero. This conclusion will be verified numerically below.

Because the initial decay follows Eq. 5, it is possible to determine the electron temperature. The value of $(D_{am})_o$ can be obtained from plots such as Fig. IX-4. If the initial temperature is independent of pressure, one obtains

$$(D_{am})_o = \frac{(D_a)_o p}{p + \dfrac{\omega_e\ \omega_i}{\nu_{ei}\ \nu_{ia}/p}}. \tag{6}$$

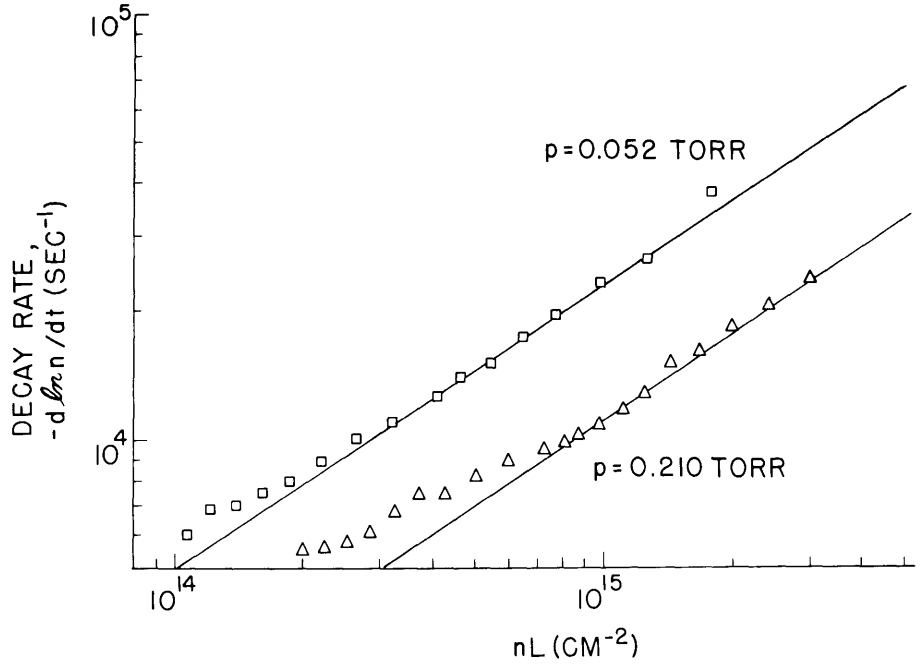

Fig. IX-4. Plasma decay rates at a magnetic field of 800 gauss. The data are fitted to lines for which $T^{3/2}/n$ is constant.

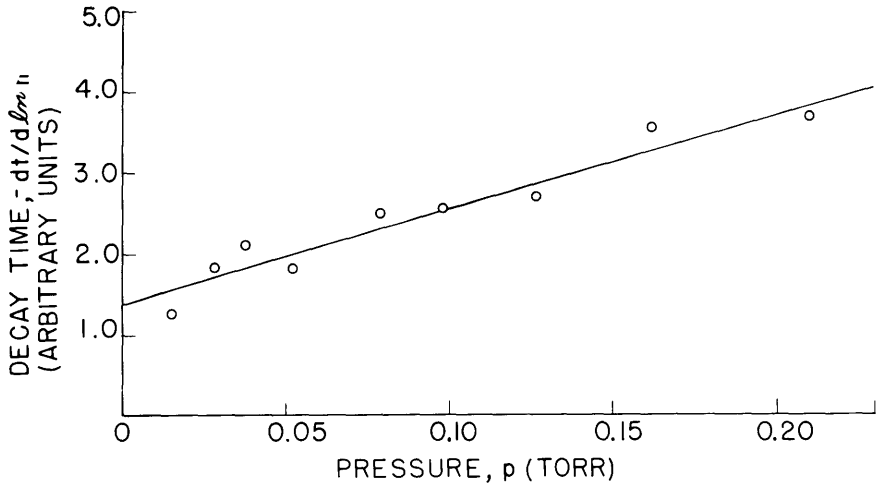

Fig. IX-5. Pressure dependence of the decay.

As the initial decay is such that ν_{ei} is constant, a plot of $(D_{am})_o^{-1}$ against p yields a straight line, as shown in Fig. IX-5. The value of ν_{ei} (and hence of T) can be obtained from this figure; it is found that at a density of 2×10^{14} cm^{-3} the temperature is 1.4 ev. The absolute diffusion rate at this density and temperature, and at a pressure

of 0.1 Torr, is 3.6×10^4 sec^{-1}, in excellent agreement with the measured decay rate (see Fig. IX-4).

Once the electron temperature is determined, it is possible to check the consistency of the approximation that Eq. 4 is zero. One finds (for example) at a pressure of 0.1 Torr, $n = 2 \times 10^{14}$ cm^{-3}, and T = 1.4 ev, that the set of terms arising from diffusion has a value $+1.0 \times 10^4$ sec^{-1}, and that the electron-ion collision term has the value -1.7×10^4 sec^{-1}. These terms thus add up to a net cooling rate of 0.7×10^4 sec^{-1}, considerably less than the initial diffusion rate. The approximation was indeed a good one. This cancellation is a fortuitous one for the experimental conditions discussed, and does not hold, for example, at a magnetic field of 400 gauss.

As the decay proceeds, the diffusion terms decrease and the collisional term remains approximately constant. Thus, after a short while the collisional term dominates the diffusion terms; in such a case the temperature can be shown[1] to drop much more rapidly than the density. Once this occurs, radiative-collisional recombination becomes important because of the strong temperature dependence of the recombination coefficient.[2] It is found that for times later than 200-300 microseconds after the start of the afterglow, the decay rates are consistent with the recombination calculations of Bates et al.[2] The bending of the decay curves of Fig. IX-4 away from the straight lines is thus apparently an indication of the onset of recombination.

Similar data was obtained at 400 gauss, although the initial temperature decay was more rapid than at 800 gauss; otherwise, the decay was qualitatively the same. At 0 gauss the temperature decays very rapidly by diffusion, and recombination becomes important almost immediately.

Detailed verification of above conclusions requires time resolved measurements of the electron temperature in addition to the electron density measurements which have been described. Temperature measurements have not been made.

E. B. Hooper, Jr.

References

1. E. B. Hooper, Jr., Ph.D. Thesis, Department of Physics, M.I.T., September 1965.
2. D. R. Bates, A. E. Kingston, and R. W. P. McWhirter, Proc. Roy. Soc. (London) A (GB), 267, 297 (1962); D. R. Bates and A. Delgarno in D. R. Bates (ed.), Atomic and Molecular Processes (Academic Press, New York, 1962).
3. E. B. Hooper, Jr. and G. Bekefi, Appl. Phys. Letters (to be published); E. B. Hooper, Jr., "Laser Interferometer," Quarterly Progress Report, No. 75, Research Laboratory of Electronics, M.I.T., October 15, 1964, p. 55; E. B. Hooper, Jr., "Electron Density Measurements with a Laser Interferometer," Quarterly Progress Report No. 78, Research Laboratory of Electronics, M.I.T., July 15, 1965, pp. 85-89.
4. V. E. Golant and A. P. Zhilinskii, Zhur. Tekh. Fiz. 32, 1313 (1962); translated in Soviet Phys. – Tech. Phys. 7, 970 (1963).

B. ION CYCLOTRON RESONANCE IN A RADIOFREQUENCY DISCHARGE – HIGH Q MODE

The ion cyclotron experiment described previously[1] has been altered slightly and, as a result, now operates in a high Q mode. This mode is strongly influenced by impurities and, thus far, has only been observed when the electrode is not oxide-coated. Alignment of the magnetic pickup probe with the electrode is another factor strongly influencing operation in this mode. The best resonance curves are obtained when the pickup is in such a position that it interferes least with the streaming of electrons along lines of $\underset{\sim}{B}_o$ from points on the electrode.

Signals from the pickup are detected by a radio receiver tuned to the applied frequency (4 Mc). The automatic volume control (AVC) voltage of the receiver is traced, as a function of B_o, on an oscilloscope face. Within experimental accuracy, the resonance occurs exactly at the ion cyclotron point

$$\beta_+ = \frac{eB_o}{M_+\omega} = 1.$$

The discharge gas is always hydrogen and only resonance of the atomic ion (proton) has been investigated.

A model has been developed[2] which accounts for a majority of effects observed. Two of the more interesting features, which are still unexplained, are:

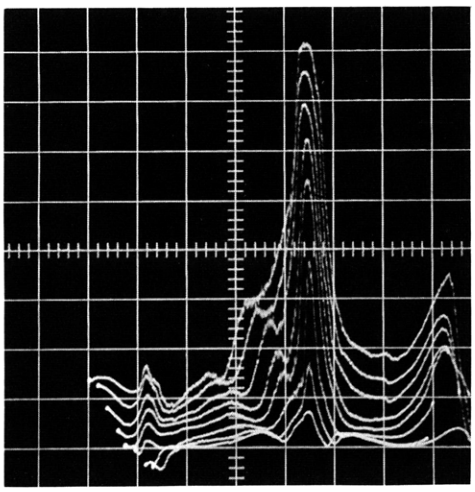

Fig. IX-6. Resonance curves at different applied voltages. Peak-to-peak applied voltage of 600 → 425 volts in steps of 25 volts. Hydrogen pressure, 18 μ.

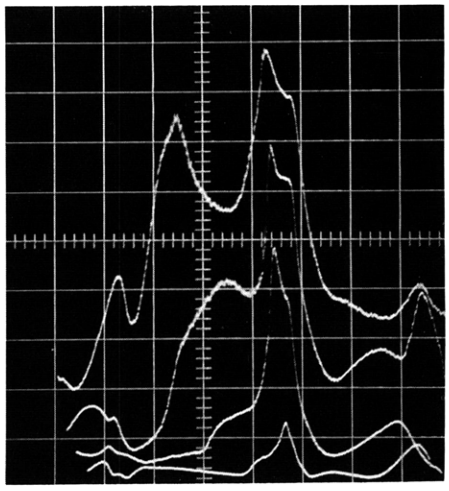

Fig. IX-7. Resonance curves at different applied voltages; 1000, 800, 600, and 500 volts peak-to-peak. Hydrogen pressure, 16 1/2 μ.

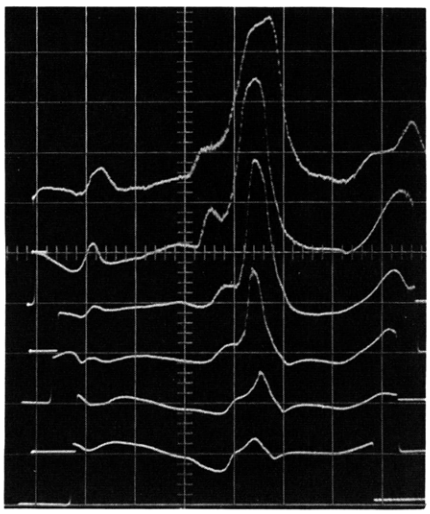

Fig. IX-8. Resonance curves at different hydrogen pressures. Pressure decreased 19 μ → 14 μ in steps of 1 μ, top to bottom. Applied voltage, 500 volts peak-to-peak.

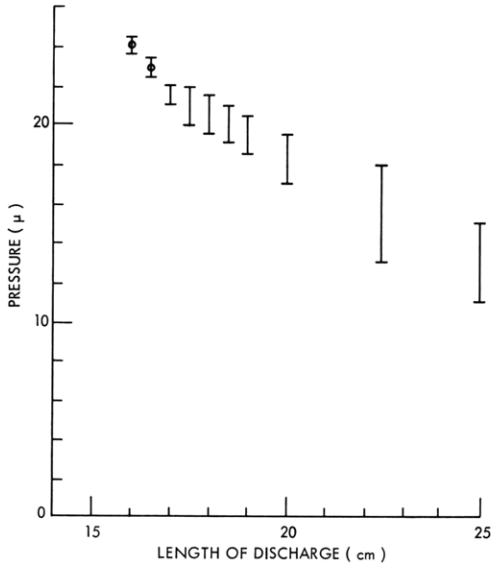

Fig. IX-9. Pressure required for observation of a sharp resonance vs length of discharge. Applied voltage, 500 volts peak-to-peak.

1. This mode is observed only when the applied RF voltage is above a certain threshold. Resonance curves are sharpest ($Q \approx 30$) just above this threshold. This is illustrated in Figs. IX-6 and IX-7.

2. This mode is observed only for a rather narrow pressure range. This pressure range is determined by the position of the (electrically insulating) end wall which limits the length of the discharge. This is illustrated in Figs. IX-8 and IX-9.

A possible explanation of these two effects is the varying percentages of atomic versus molecular ions and neutral particles. This matter requires further investigation.

J. J. Nolan, Jr.

References

1. J. J. Nolan, Jr., "Ion Cyclotron Resonance in a Radiofrequency Discharge," Quarterly Progress Report No. 77, Research Laboratory of Electronics, M. I. T., April 15, 1965, pp. 109-112.

2. J. J. Nolan, Jr., "'Direct Coupling' to a Plasma in the Vicinity of Ion Cyclotron Resonance," Ph. D. Thesis, Department of Electrical Engineering, Massachusetts Institute of Technology, September 1965.